

PROCEEDINGS OF SPIE

[SPIDigitalLibrary.org/conference-proceedings-of-spie](https://spiedigitallibrary.org/conference-proceedings-of-spie)

Lidar measurements of airborne particulate matter

Guangkun Li, C. Russell Philbrick

Guangkun Li, C. Russell Philbrick, "Lidar measurements of airborne particulate matter," Proc. SPIE 4893, Lidar Remote Sensing for Industry and Environment Monitoring III, (21 March 2003); doi: 10.1117/12.466128

Event: Third International Asia-Pacific Environmental Remote Sensing
Remote Sensing of the Atmosphere, Ocean, Environment, and Space, 2002,
Hangzhou, China

SPIE.

Lidar measurements of airborne particulate matter

Guangkun Li and Russell Philbrick

The Pennsylvania State University, Department of Electrical Engineering,
University Park, PA 16802

ABSTRACT

Raman lidar techniques have been used in remote sensing to measure the aerosol optical extinction in the lower atmosphere, as well as water vapor, temperature and ozone profiles. Knowledge of aerosol optical properties assumes special importance in the wake of studies strongly correlating airborne particulate matter with adverse health effects. Optical extinction depends upon the concentration, composition, and size distribution of the particulate matter. Optical extinction from lidar returns provide information on particle size and density. The influence of relative humidity upon the growth and size of aerosols, particularly the sulfate aerosols along the northeast US region, has been investigated using a Raman lidar during several field measurement campaigns. A particle size distribution model is being developed and verified based on the experimental results. Optical extinction measurements from lidar in the NARSTO-NE-OPS program in Philadelphia PA, during summer of 1999 and 2001, have been analyzed and compared with other measurements such as PM sampling and particle size measurements.

KEYWORDS: LIDAR, OPTICAL EXTINCTION, PARTICULATE MATTER

1. Introduction

Lidar techniques have been used to make remote sensing measurements of the aerosol optical extinction together with other atmospheric optical scattering properties of the molecular species. Recent studies have associated increases in airborne particulate matter with increased morbidity and mortality, particularly in elderly and respiratory impaired individuals. Knowledge of aerosol optical properties assumes special importance in the wake of studies strongly correlating airborne particulate matter with adverse health effects.^{1,2} The small aerosol component, labeled PM_{2.5}, made up of particles with aerodynamic size less than $2.5 \mu\text{m}$, is of most concern to human health because these can be easily inhaled deep into the lungs. Along with health issues, aerosol particle distributions have significant implications for natural environment aesthetics and climatic change conditions.³ Increases in aerosol loading in the atmosphere can lead either to an increase or decrease in the mean global temperature of Earth, because their optical properties in the visible and infrared portion of the spectrum depend on the size distributions of aerosols. Additionally, airborne particle distributions have significant influence on the visibility that effects scheduled aircraft traffic.^{4,5}

2. LAPS Raman Lidar Instrument

Lidar techniques using molecular Raman scattering provide a useful method for studying the atmosphere properties and constituents. A lidar system transmits a laser pulse at a certain wavelength into the atmosphere and a telescope collects the returned signals, which include direct backscatter, as well as vibrational Raman and rotational Raman signals. Several of these wavelengths are measured corresponding to the primary molecular species and the airborne particles. These return signals are then analyzed to obtain profiles of atmospheric constituents, temperature and optical extinction. We have used Raman lidar and backscatter lidar techniques to measure the optical extinction and scattering properties as part of the NARSTO-NE-OPS (NorthEast-Oxidant and Particle Study) during the summers of 1998, 1999 and 2001.⁶

LAPS (Lidar Atmospheric Profile Sensor) instrument transmits at both the 2nd and 4th harmonics of a 1064-nm Nd:YAG laser, at 532 nm and 266 nm, respectively. The return signals are measured by photo-multiplier tubes (PMT's), operated in photon counting mode after the signals are spectrally separated and isolated. The intensity of light is measured at

seven frequency shifted Raman scatter wavelengths, which are listed in Table 1. Table 2 gives information about the sub-systems that make up the LAPS lidar instrument.

LAPS is capable of measuring vertical profiles of water vapor, temperature, ozone, visible optical extinction from the 532 transmitted signal, and ultraviolet optical extinction from the 266 transmitted signal.^{7,8} Table 1 lists the LAPS wavelengths which include the rotational Raman backscatter signals at 530 and 528 nm and the vibrational Raman scatter signals at 660, 607, 277, 284 and 295 nm. A measurement of the atmosphere ozone density is obtained by measuring the departure from the constant mixing ratio of oxygen and nitrogen using the vibrational Raman shifts of O₂ at 277 nm and N₂ at 284nm that occur on the steep side of the Hartley band of ozone absorption. The measurement sensitive to atmosphere temperature is obtained by taking the ratio of the rotational Raman signals at 528 and 530 nm. A measurement of water vapor is obtained by taking the ratios of the water vapor to nitrogen determined from the vibrational Raman signals at 660/607nm and 295/284 nm. Additional correction is needed for water vapor determined from the ratio of 295/284 nm due to ozone absorption. Optical extinction, which is a measure of the total attenuation of a laser beam due to scattering and absorption, is determined by differentiation of the profiles of Raman scatter return signals at 607, 530 and 284nm.⁸

Table 1. Measurements made by the LAPS lidar instrument

Property	Measurement	Altitude	Time Resolution
Water Vapor	660/607 Raman 294/285 Raman	Surface to 5 km Surface to 3 km	Night - 1 min. Day & Night - 1 min.
Temperature	528/530 Rotational Raman	Surface to 5 km	Night 30 min.
Ozone	276/285 Raman/DIAL	Surface to between 2 and 3 km	Day and Night 30 min.
Optical Extinction at 530 nm	530 nm Rotational Raman	Surface to 5 km	Night 10 to 30 min.
Optical Extinction at 607 nm	607 N ₂ 1 st Stokes	Surface to 5 km	Night 10 to 30 min.
Optical Extinction at 285 nm	285 N ₂ 1 st Stokes	Surface to 3 km	Day and Night 30 min.

Table 2. LAPS Lidar characteristics

Transmitter	Continuum 9030 -- 30 Hz 5X Beam Expander	600 mj @ 532 nm 130 mj @ 266 nm
Receiver	61 cm Diameter Telescope	Fiber optic transfer
Detector	Seven PMT channels Photon Counting	528 and 530 nm -- Temperature 660 and 607 nm -- Water Vapor 294 and 285 nm -- Daytime Water Vapor 276 and 285 nm -- Raman/DIAL Ozone
Data System	DSP 100 MHZ	75 meter range bins
Safety Radar	Marine R-70 X-Band	protects 6° cone angle around beam

3. Optical Extinction from Raman Lidar

Previous remote sensing instruments, whether using lasers, radars, or microwaves, have had difficulties determining actual extinction profile from backscatter signals. This is due to the large variations in the relative contributions of backscatter and extinction due to particles of different size distributions along the propagation path. However, the molecular profiles from the Raman scatter signals provide direct measurements of the optical extinction. The inelastic Raman backscatter signal is affected by aerosol extinction but not by aerosol backscatter, and thus Raman Lidar provides the capability to profile the optical extinction.

The LAPS instrument uses the molecular scattering properties of the species in the lower atmosphere to simultaneously measure profiles of ozone, water vapor, temperature, and optical extinction. The optical extinction profiles are obtained from the gradients in the vertical profiles of the rotational Raman molecular signal at 530nm and the N₂ vibrational Raman signals measured at 284 and 607nm. The wavelength dependence of the optical extinction from both ultraviolet and visible channels can be used to interpret the changes in the particle size distribution as a function of altitude for the aerosol components of the atmosphere, after removing the known molecular component. Also, these measurements can be used to determine the air mass parameter and atmospheric optical depth.

In order to calculate extinction due to aerosols from Raman lidar measurements, an algorithm has been developed for calculation from Raman lidar equation.⁹ The Raman lidar equation can be written as,

$$P(\lambda_R, z) = E_T(\lambda_T) \xi_T(\lambda_T) \xi_R(\lambda_R) \frac{c\tau}{2} \frac{A}{z^2} \beta(\lambda_T, \lambda_R) \exp\left[-\int_0^z [\alpha(\lambda_T, z') + \alpha(\lambda_R, z')] dz'\right], \quad (1)$$

where z is the altitude of the volume element, λ_T is the wavelength transmitted, λ_R is the wavelength received, $E_T(\lambda_T)$ is the energy per laser pulse transmitted at wavelength λ_T , $\xi_T(\lambda_T)$ is the net optical efficiency at wavelength λ_T of all transmitting elements, $\xi_R(\lambda_R)$ is the net optical efficiency at wavelength λ_R of all receiving elements, c is the speed of light, τ is the time duration of the laser pulse, A is the area of the receiving telescope, $\beta(\lambda_T, \lambda_R)$ is the back scattering cross section of the volume element for the laser wavelength, λ_T , at Raman shifted wavelength, λ_R , and $\alpha(\lambda, z')$ is the extinction coefficient at wavelength, λ , at range z' . For vibrational Raman scattering, the backscatter coefficient $\beta(\lambda_T, \lambda_R)$ can be shown to be,

$$\beta(\lambda_T, \lambda_R, z) = N_i(z) \left\{ \frac{d\sigma(\lambda_T, \lambda_R, \pi)}{d\Omega} \right\}_i, \quad (2a)$$

where $N_i(z)$ represents the number density of species i , and $\left\{ \frac{d\sigma(\lambda_T, \lambda_R, \pi)}{d\Omega} \right\}_i$ is the differential Raman backscatter cross-section of the gas of molecular species i . The species i can be nitrogen, oxygen or water vapor depending on the received wavelength of the Raman scatter signal.

Because all of the molecules of the lower atmosphere are distributed in the rotational states according to their temperature, the wavelength distribution of the rotational signal can be used to measure the temperature profile. For rotational Raman scattering, the backscatter coefficient $\beta(\lambda_T, \lambda_R)$ can be shown to be,

$$\beta(\lambda_T, \lambda_R, z) = N(z) \left\{ \frac{d\sigma(\lambda_T, \lambda_R, \pi)}{d\Omega} \right\}, \quad (2b)$$

where $N(z)$ represents the number density of all the molecules and $\left\{ \frac{d\sigma(\lambda_T, \lambda_R, \pi)}{d\Omega} \right\}$ is the differential Raman backscatter cross section of the rotational Raman shift at wavelength λ_R . The rotational Raman signal near the top of the distribution of states, that occurs near 530 nm, is not very dependent upon temperature. Thus this wavelength's signal provides an excellent molecular profile, which can be used to determine the optical extinction.⁸ The LAPS Raman lidar is used to calculate optical extinction at three wavelengths, 284 nm, 530 nm and 607 nm, where the 284nm and 607nm

profiles are derived from the Raman shift of nitrogen scattering of beams generated using the 2nd and 4th harmonics of the Nd:YAG, and the 530nm wavelength is from the rotational Raman scattering of the 2nd harmonic.

Since the number density of nitrogen is a well known fraction of the atmospheric molecules, it can represent the number density of all the molecules in atmosphere. It follows from Equations (1), (2a), and (2b) that,

$$\alpha(\lambda_T, z) + \alpha(\lambda_R, z) = \frac{d}{dz} \left[\ln \frac{F(z)N(z)}{z^2 P(z)} \right] \quad (3)$$

λ_R is the Raman shift wavelength at 284, 530 and 607nm, $N(z)$ is the total molecular number density, $F(z)$ is the telescope overlap function. The extinction coefficients in equation (3) can be written as,

$$\alpha(\lambda_T, z) + \alpha(\lambda_R, z) = \alpha_{\lambda_T}^{mol-sca}(z) + \alpha_{\lambda_T}^{aer-sca}(z) + \alpha_{\lambda_R}^{mol-sca}(z) + \alpha_{\lambda_R}^{aer-sca}(z) + \alpha_{\lambda_T}^{abs}(z) + \alpha_{\lambda_R}^{abs}(z) \quad (4)$$

where $\alpha_{\lambda}^{mol-sca}(z)$ and $\alpha_{\lambda}^{aer-sca}(z)$ are the extinction coefficients due to molecular and aerosol scattering of the atmosphere at the transmit and receive wavelengths, and α_{λ}^{abs} is molecule and aerosol extinction coefficient due to optical absorption. The ozone absorption coefficient is an important factor contributing to the total extinction calculation at the ultraviolet wavelength 284 nm. Absorption by molecules is considered to be negligible at the mid-visible wavelengths of 532 nm and 607 nm in these extinction calculations.

The molecular extinction coefficients for 284, 530 and 607nm are known from the scattering cross-sections for N₂ and O₂. The overlap function $F(z)$ is equal to 1 where the path of the beam is within the field-of-view of the receiver above an altitude of 800 meters for the LAPS instrument. If we assume a wavelength dependence of the aerosol extinction, such as a linear equation,

$$\frac{\alpha_{\lambda_T}^{aer}}{\alpha_{\lambda_R}^{aer}} = \frac{\lambda_R}{\lambda_T} \quad (5)$$

The linear response is a first order approximation to the aerosol wavelength dependence case for extinction measurements. The aerosol extinction coefficient at 530nm then can be written as,

$$\alpha_{\lambda_R}^{aer} = \frac{\frac{d}{dz} \left[\ln \frac{N(z)}{P(z)z^2} \right] - \alpha_{\lambda_T}^{mol}(z) - \alpha_{\lambda_R}^{mol}(z)}{1 + \frac{\lambda_T}{\lambda_R}} \quad (6a)$$

$$\approx \frac{\frac{d}{dz} \left[\ln \frac{N(z)}{P(z)z^2} \right] - \alpha_{\lambda_T}^{mol}(z) - \alpha_{\lambda_R}^{mol}(z)}{2}$$

where the difference due to the wavelengths being at 530 and 532nm are considered to be negligible.

The aerosol extinction coefficient at 607nm can be written as:

$$\alpha_{\lambda_R}^{aer} \approx \frac{\frac{d}{dz} \left[\ln \frac{N(z)}{P(z)z^2} \right] - \alpha_{\lambda_T}^{mol}(z) - \alpha_{\lambda_R}^{mol}(z)}{1.88} \quad (6b)$$

The 607 and 530 nm wavelengths are widely separated, however, since the extinction coefficient at 530nm can be first determined, there is no need to assume a wavelength dependence for the aerosol scattering.

For the 284 nm channel, the absorption coefficient at the transmit wavelength of ultraviolet wavelength is significant due to ozone absorption. To calculate the aerosol extinction coefficient, we have developed a method to measure the ozone density profile using the LAPS instrument and include the ozone absorption at in transmit and receive wavelengths. Also, the extinction coefficient at 284nm, which includes aerosol scattering and ozone absorption, can be approximated as,

$$\alpha_{\lambda_R}^{aer} \approx \frac{\frac{d}{dz} \left[\ln \frac{N(z)}{P(z)z^2} \right] - \alpha_{\lambda_T}^{mol}(z) - \alpha_{\lambda_R}^{mol}(z) - \alpha_{\lambda_T}^{ozone}(z) - \alpha_{\lambda_R}^{ozone}(z)}{1.94} \quad (6c)$$

The telescope form factor is introduced to correct the received signal profile at the low altitudes where the out-of-focus ray bundle overfills the detector.¹⁰ The near field rays overfill the end of the fiber, which then acts as an aperture stop, and requires a range dependent form factor to correct the shape of the lower altitude profile. Both the geometrical overlap correction method and an experimental approach have been tested to solve this problem. In this analysis, attention is direct to the experimental solution due to its straightforward application. The experimental approach requires a time period with the weather conditions as clear and dry as possible. Under clear conditions, where the aerosol extinction and backscattering are relatively small, the laser return signal will vary exponentially with the altitude. We can accurately predict the desired lidar return signal profile during these periods, and then calculate the telescope form factor.

4. Results and Analysis

Figure 1 shows a plot of extinction profiles due to aerosol and molecule scattering at each wavelength measured during the night on 21 August 1998. The profiles were obtained in the NE-OPS pilot study at a time when the atmosphere was relatively clean. Error bars are included to show the standard deviation of the measurements. The aerosol scattering optical extinction profiles at the visible wavelengths of 530 nm and 607 nm exhibit similar profile shapes, with the 607nm extinction being slightly smaller. The extinction values at the visible wavelength are much smaller than those values at ultraviolet wavelength because of the larger scattering cross-section of ultraviolet wavelengths for molecules and small particles.

Figure 2 shows the relative differences when a selected sample distribution is presented as atmosphere particle size radius, surface area, and volume distributions. It has been suggested that multi-model log-normal distributions be chosen as representative of most dusts.¹¹ The surface area distribution ($dS/d\log r$) and volume density distribution ($dV/d\log r$) are most important for the study of optical scattering properties of particles and the mass concentration in atmosphere, respectively. As shown in Figure 2, the largest number of particles are found at smaller sizes in the range of nuclei mode, which is around 10 nm. The large particles measurements are often reported as the summation of all particles of aerodynamic size less than 10 μm , PM_{10} , or less than 2.5 μm , $\text{PM}_{2.5}$. Typical airborne particle distributions which most effect the optical extinction are particles in the range 0.02-0.4 μm (accumulation mode particles).

LAPS Raman lidar measurements provide remotely measured profiles of atmospheric constituents, as well as a picture of the dynamics of the atmosphere. Figure 3, 4 and 5 show examples of time sequence of profiles measured by the LAPS lidar. Time sequence plots of vertical profiles of extinction provide a description the horizontal and vertical structure as the atmosphere advects past the vertical beam during a period of time. A time sequence of profiles on 5 September 1996 shows extinction at ultraviolet and visible wavelengths in Figure 3 (a) and (b). Figure 3(c) and (d) show the time sequence plots of ozone concentration and water vapor mixing ratio measured by LAPS at the same time as the extinction profiles. A 500 meters thick sub-visual cloud layer at height 2 km can be seen in the extinction plots of both ultraviolet and visible wavelengths beginning about 0200 UTC. The average value of extinction coefficient at 530 nm is about 0.25 km^{-1} , which corresponds to about 88% transmittance through a 500m thick layer. This layer would probably not be observed visually, but it is easily detected by the lidar instrument. The extinction value for the ultraviolet channel is much larger than the visible channel in this cloud layer. Further discussion of this feature follows. In Figure 6(a) we show the ratio of extinction efficiency calculated at 284nm and 530 nm as the particle size changes, for a transparent sphere. Two kinds of particles are presented in the figure, non-absorbing particles with reflective index 1.55 and particles with reflective index $1.55+0.01i$. For fine non-absorbing particles, which are smaller than 20 nm in size, the ratio between wavelengths 284nm and 530nm is approximately 10, and for coarse mode particles, the ratio of these two wavelengths falls to unity as the size increases. This variance is very useful to indicate when we consider the variations in particle size in atmosphere. Figure 6(b) shows the measurements of the vertical profiles of extinction at these two wavelengths. As shown, the ratio of ultraviolet to visible extinction is about inside the cloud, which implies that the sub-visual cloud is formed by small particles, probably indicating the early formation of a cloud.

Additional comparisons of SCOS 97 measurements of the extinction ratio of ultraviolet to visible wavelengths are shown in Figures 4 and 7. Figure 7 shows a cloud layer at height about 4.5 km, the cloud layer is also observed in Figure 4 from time sequence plots of both ultraviolet and visible wavelengths. The values of extinction coefficient of the two wavelengths within the cloud are nearly the same with a ratio close to unity. This result indicates that the cloud layer is formed by large coarse mode particles.

The fact that extinction has a strong correlation with relative humidity has been observed in a number of data sets. It has been established that there is a sharp change in extinction at a threshold relative humidity of 80%. The lidar is most sensitive to particle sizes in the accumulation mode, which is formed as ultra fine particles grow to form larger particles ($>0.2\mu\text{m}$). One method for particles to grow depends on high relative humidity and is effective above critical saturation ratio of the particle. Water vapor content and temperature are the important factors in determining the optical extinction because of the relative humidity determines the equilibrium size distribution, and thus determines the optical extinction. Ground level extinction from the 284 nm channels for various periods was analyzed and compared to relative humidity to determine the correlation of extinction and relative humidity, see Figure 5 and Figure 8. Figure 5 show the time sequence of vertical profiles of extinction and water vapor, respectively. Figure 5a shows a sudden increase of extinction at the surface during the night of 3 July 1999, which is due to formation of a fog layer near ground. However, the ground water vapor mixing ratio is very uniform at the same time, which is shown in Figure 5b. Figure 8 shows the corresponding increase and decrease in extinction as the relative humidity rises and falls through the threshold of 80 % at the same time period. It may indicate that the increase of extinction is corresponding to the increase of particle size due to condensation of water vapor.

Comparison of measurements of extinction and particulate matter are shown in Figure 9. Figure 9a shows the PM measurements using the Millersville University tethered sonde at altitude 100m, 200m, 300m and at the surface.¹³ The results in Figure 9a show two different conditions that are frequently observed in the nocturnal boundary layer. In one case, several thin layers are observed to drift through the region and strong vertical gradients in the particle layers are observed. In the second case, during a very calm period, a fog layer is formed below 200 m, which is a similar condition to that shown in Figures 5 and 8. In Figure 9b, both the lidar extinction and dry mass of particulate matter were averaged for 60 minute periods in these presentations. The surface level particulate matter measurement was measured by Harvard School of Public Health.¹⁴ The lidar extinction measurements near the surface have a large error below 800 meters due to the telescope form factor and so the extinction measurements at 800 meters are compared to the surface measurements of PM_{2.5} under the assumption that the atmospheric boundary layer is uniform. Of This comparison serves to show the relationship between the PM and the optical extinction. The strong correlation between optical extinction and PM concentration is clearly demonstrated.

5. Conclusion

Lidar has the capability of measuring vertical profiles of meteorological conditions and atmospheric optical properties at the same time. This capability provides a much more useful measure of atmospheric structure than previous approaches. The wavelength dependence of the optical extinction from both ultraviolet and visible channels can be used to detect the changes in the particle size distribution as a function of altitude. Optical extinction and hence particle size distribution exhibit a sharp increase when the relative humidity goes above 80 % and decreases again when the humidity goes below 80 %, thus demonstrate that optical extinction and relative humidity are strongly correlated for these aerosols. The wavelength dependence of optical extinction can be used to detect changes in particle size, as a function of time and altitude. These results show a strong correlation observed between extinction measured from lidar and surface PM mass concentrations. The lidar results can be used to describe the vertical distribution of the airborne particulate matter. Results from using the lidar then provided a more accurate description of the evolution of air pollution episodes. The vertical distributions of airborne particulate matter, which can be measured by Raman lidar, are expected to provide a critical test for the evaluation and development of air quality models.

6. References

1. Albritton, Daniel L., and Daniel S. Greenbaum: 1998, "Atmospheric Observations: Helping Build the Scientific Basis for Decisions Related to Airborne Particle Matter," *Proceedings of the PM Measurements Research Workshop*, Chapel Hill, North Carolina, July 22-23.
2. Hidy, G. M., P. M. Roth, J. M. Hales and R. Scheffe: 1998, Oxidant Pollution And Fine Particles: Issues And Needs. *NARSTO Critical Review Series*.
3. Seinfeld, J.H and S.N, Pandis: 1998. *Atmospheric Chemistry and Physics: From Air Pollution to Climate Change*, Wiley-Interscience
4. Kyle T.G.: 1991. *Atmospheric Transmission: Emission & Scattering*, Butterworth-Heinemann
5. National Academy: 1998. *The Atmosphere Science: Entering the Twenty-First Century*, National Academy Press.
6. Philbrick, C. R.: 1998, Investigations of Factors Determining the Occurrence of Ozone and Fine particles in Northeastern USA. *Meas. of Toxic and Related Air Pollutants*. 1:248-260.
7. Philbrick, C. R.: 1998, Raman Lidar capability to measure Tropospheric Properties. *Proceedings of the Nineteenth International Laser Radar Conference*, NASA Langly Research Center, Hampton VA, NASA Conf. Publ. 207671, p289 – 292.
8. Philbrick, C. R.: and D.B. Lysak: 1998, Atmospheric Optical Extinction Measured by Lidar. *NATO-RTO Meeting Proceedings I, E-O Propagation, Signature and System Performance Under Adverse Meteorological Conditions*. 40:1-7.
9. Measures, R.:1992, *Laser Remote Sensing-Fundamentals and Applications*. Krieger.
10. J. R. Jenness, D. B. Lysak, and Philbrick C.R. :1997, Design of a Lidar Receiver with Fiber-optic Output. *Applied Optics*. 36:4278.
11. Kelkar, D.N. and P.V. Joshi: 1977, "A Note on the Size Distribution of Aerosols in Urban Atmospheres", *Atmospheric Environment*, Vol. 11, pp. 531-534.
12. Ansmann, A., U. Wandinger, M. Riebesell, C. Weitkamp, and W. Michaelis :1992, Independent Measurement of Extinction and Backscatter Profiles in Cirrus Clouds by using a Combined Raman Elastic-Backscatter Lidar. *Applied Optics*. 31:7113.
13. Private communication of sonde measurements conducted by Prof. Richard Clark, Millersville University.
14. Private communication of PM₁₀ and PM_{2.5} measurements conducted by George Allen, Harvard School of Public Health.

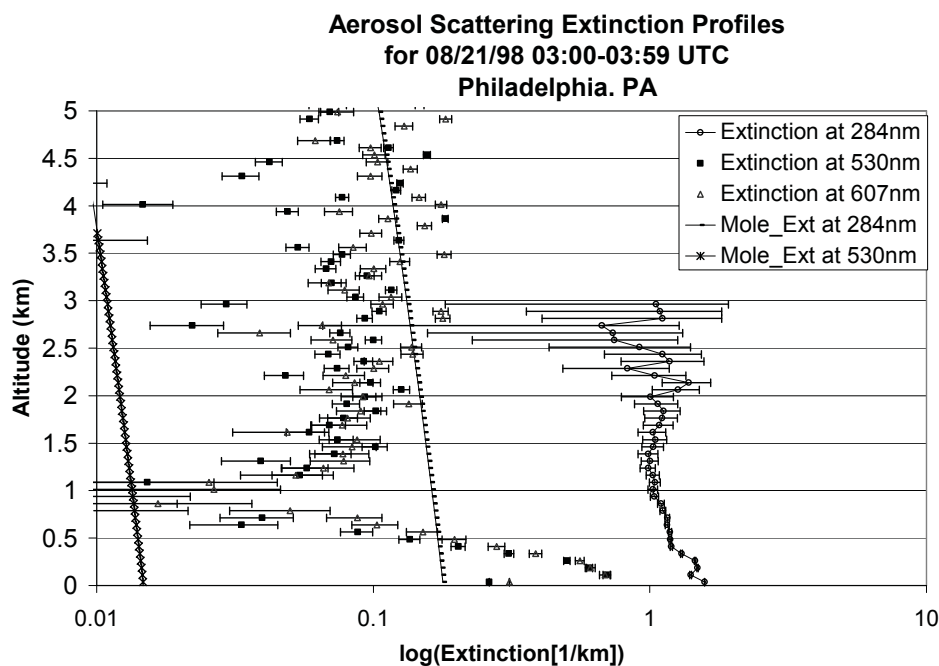


Figure 1. Integration of vertical extinction profiles at wavelengths 284, 530 and 607 nm for 60 minutes during the NE-OPS 98 campaign.

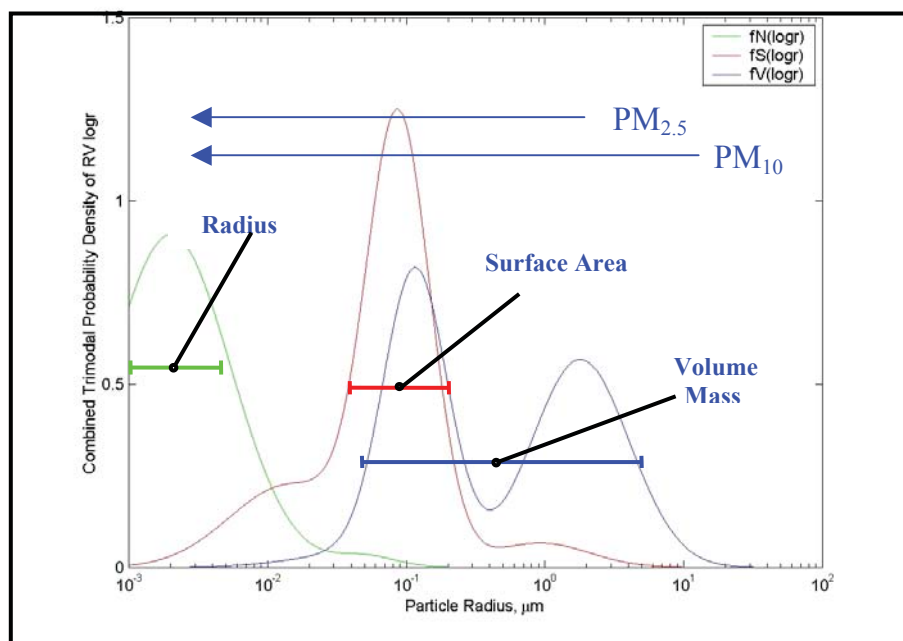


Figure 2. Description of airborne particles depends on measurement parameters, radius, surface area, and volume, where represents number density, optical scattering, mass; Optical measurements are most sensitive to area for particles 0.02-0.5 μ m (accumulation mode particles).

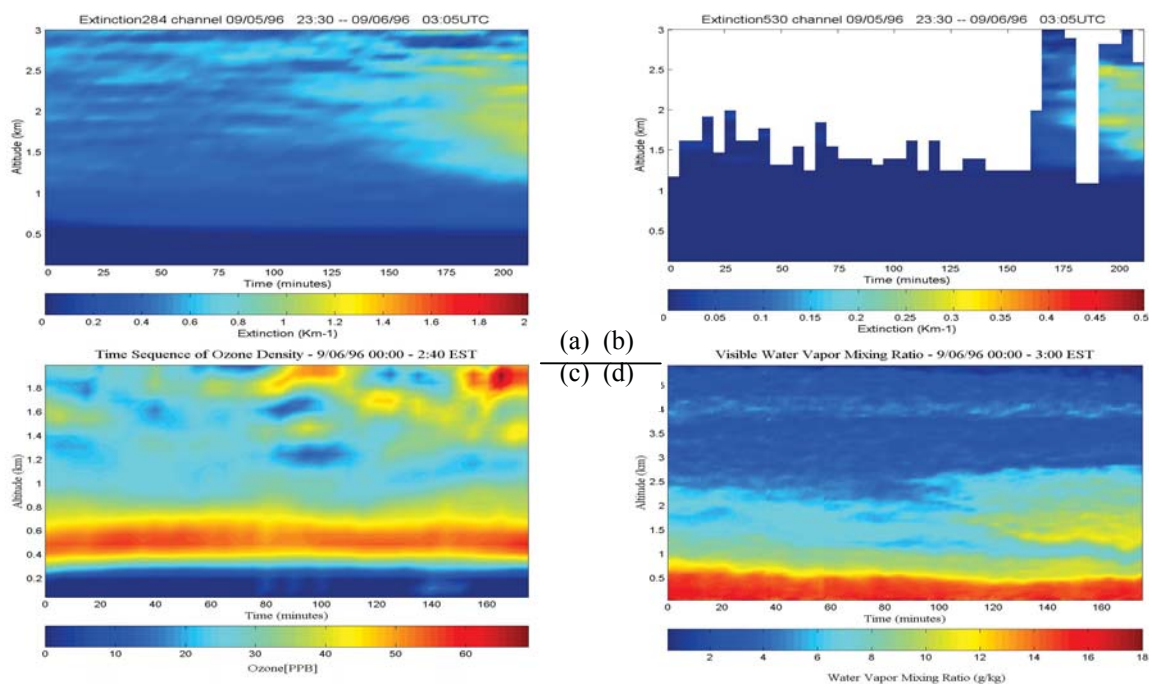


Figure 3. Time sequence plots of extinction at wavelength of (a) 284nm , (b) 530nm and (c) ozone concentration and (d) water vapor mixing ratio during summer 23:30 05/96 – 03:05 06/96 UTC.

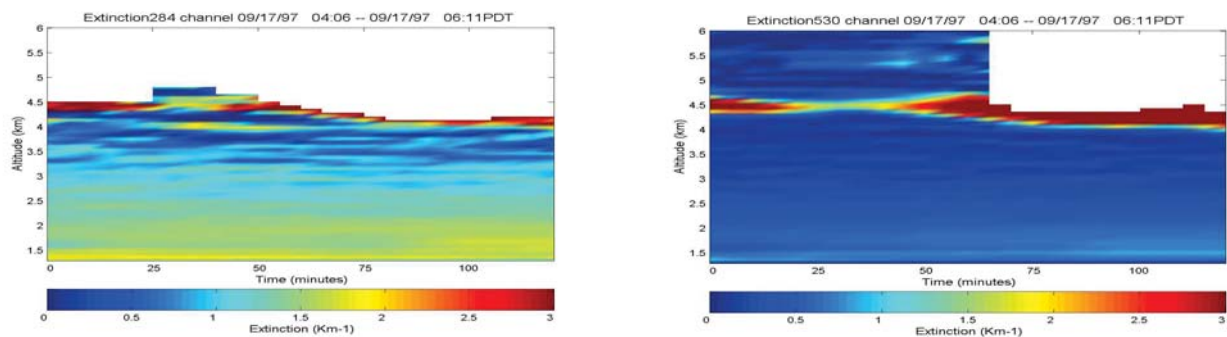


Figure 4. Time sequence and integrated profiles of optical extinction – SCOS 97 (a) Time sequence of extinction at 284nm; (b) Time sequence of extinction at 530nm.

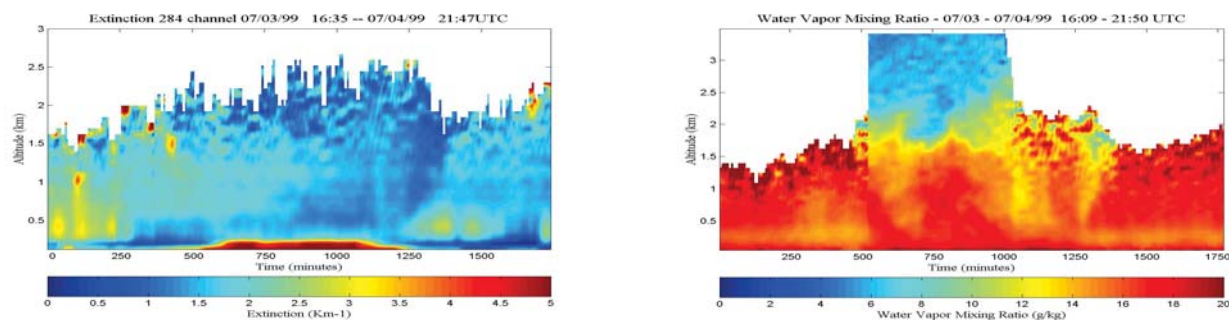


Figure 5. (a) Time sequence vertical extinction (b) Water vapor mixing ratio during NE-OPS 08/01/99 01:10 – 08/02/99 00:40 UTC

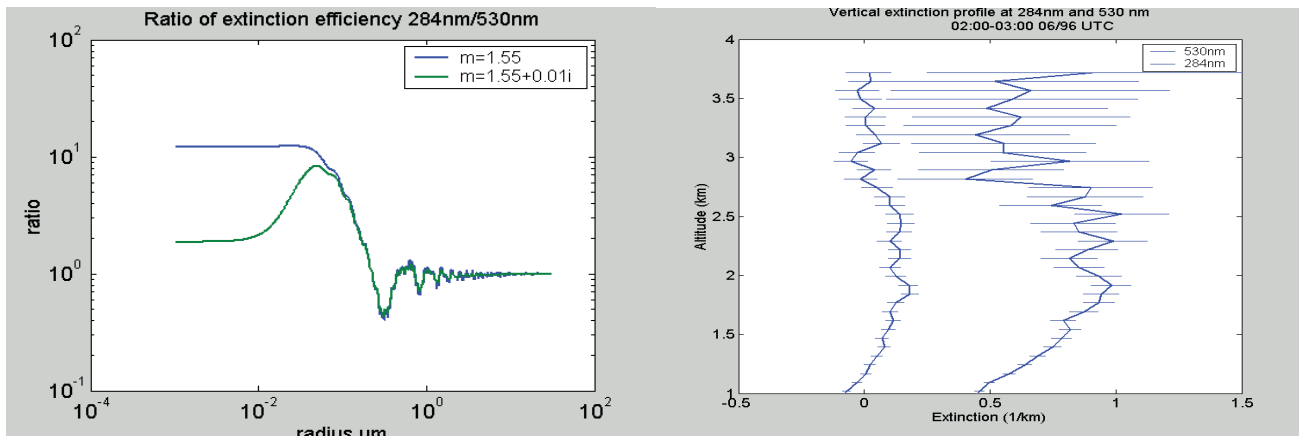


Figure 6. (a) Ratio of extinction efficiency of 284nm/530 nm. (b) Integration of vertical extinction profiles at wavelengths 284, 530 and 607 nm for 60 minutes during the time 02:00-03:00 09/06/96 UTC, which is from the result in Figure 3.

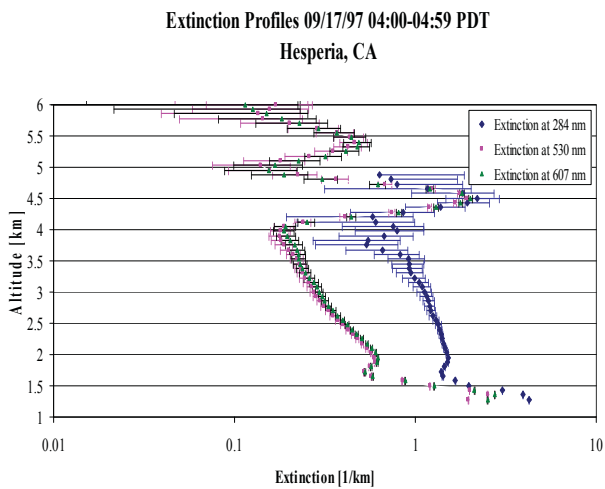


Figure 7. Integration of vertical extinction profiles at wavelengths 284, 530 and 607 nm for 60 minutes during SCOS 97 04:00 -05:00 09/17/97 UTC, which is from the result in Figure 4.

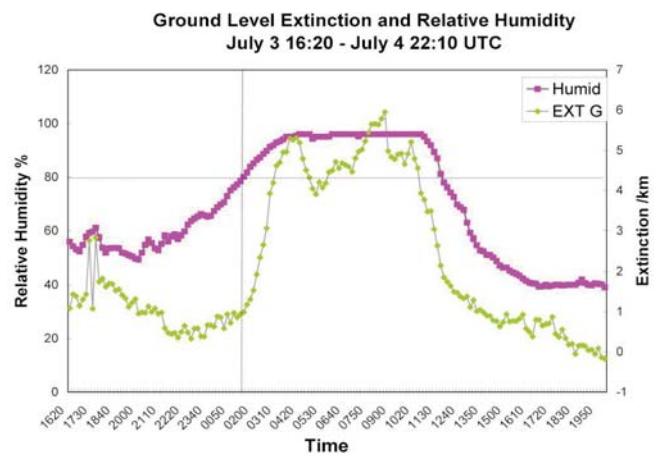
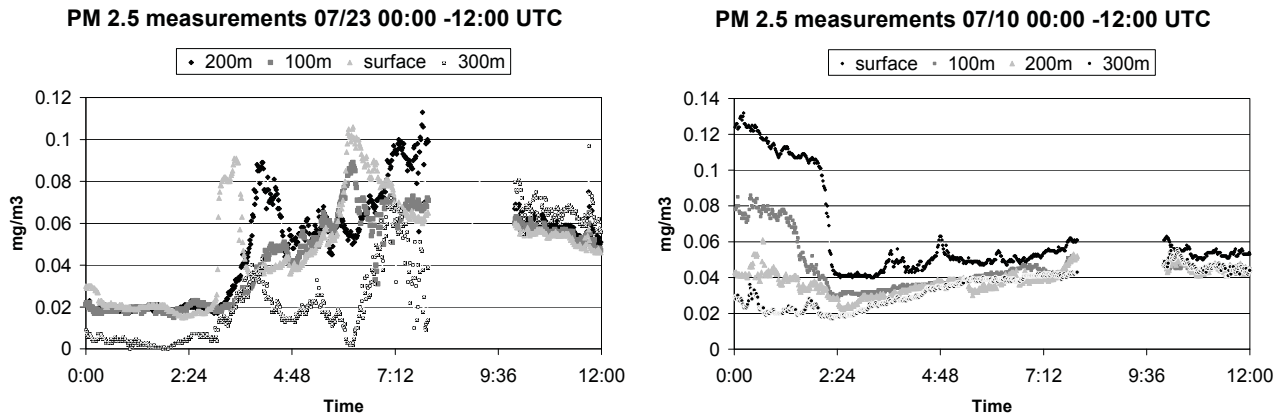
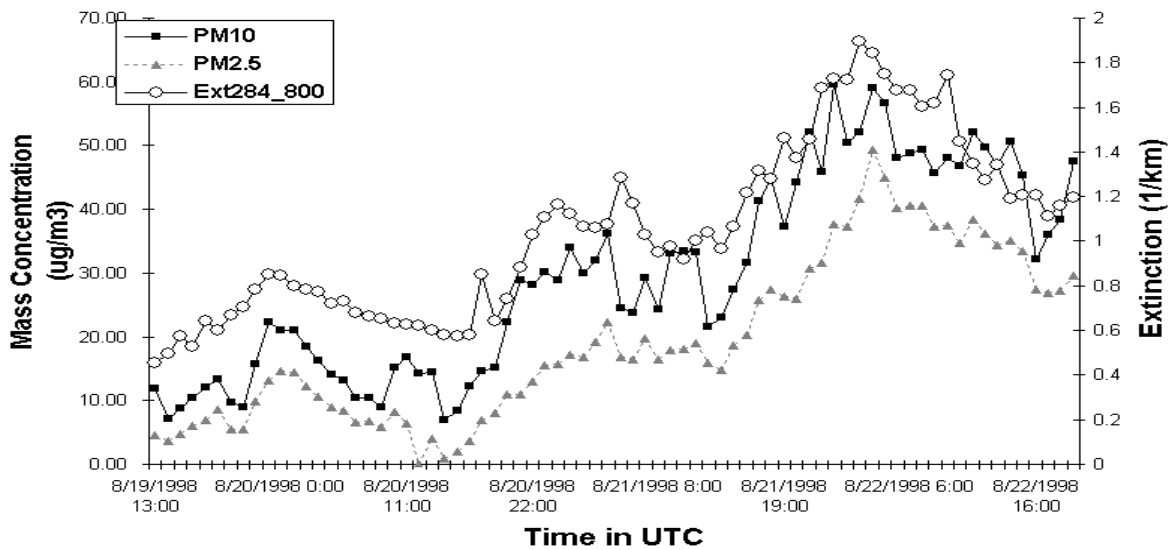


Figure 8. Comparison of ground level extinction and relative humidity during NE-OPS 99, which is corresponding to the results in Figure 5.



(a)

Time sequence of Extinction at 800 m and PM2.5 and PM 10 from Aug. 19 to Aug. 22 of 1998



(b)

Figure 9. (a) Tethered Sonde Data (Richard Clark Millersville University). Comparison of PM measurements from Tethered Sonde at surface and at altitude 100m, 200m, and 300m. (b) Comparison of PM concentration with Extinction at 284 nm, August 15 to August 22, 1998.